

## Development and validation of a drinking water temperature model in domestic drinking water supply systems

Zlatanović, Ljiljana; Moerman, A.; van der Hoek, Jan Peter; Vreeburg, Jan; Blokker, M

**DOI**

[10.1080/1573062X.2017.1325501](https://doi.org/10.1080/1573062X.2017.1325501)

**Publication date**

2017

**Document Version**

Final published version

**Published in**

Urban Water Journal

**Citation (APA)**

Zlatanović, L., Moerman, A., van der Hoek, J. P., Vreeburg, J., & Blokker, M. (2017). Development and validation of a drinking water temperature model in domestic drinking water supply systems. *Urban Water Journal*, 14(10), 1031-1037. <https://doi.org/10.1080/1573062X.2017.1325501>

**Important note**

To cite this publication, please use the final published version (if applicable). Please check the document version above.

**Copyright**

Other than for strictly personal use, it is not permitted to download, forward or distribute the text or part of it, without the consent of the author(s) and/or copyright holder(s), unless the work is under an open content license such as Creative Commons.

**Takedown policy**

Please contact us and provide details if you believe this document breaches copyrights. We will remove access to the work immediately and investigate your claim.



## Development and validation of a drinking water temperature model in domestic drinking water supply systems

Ljiljana Zlatanovic, Andreas Moerman, Jan Peter van der Hoek, Jan Vreeburg & Mirjam Blokker

To cite this article: Ljiljana Zlatanovic, Andreas Moerman, Jan Peter van der Hoek, Jan Vreeburg & Mirjam Blokker (2017) Development and validation of a drinking water temperature model in domestic drinking water supply systems, Urban Water Journal, 14:10, 1031-1037, DOI: [10.1080/1573062X.2017.1325501](https://doi.org/10.1080/1573062X.2017.1325501)

To link to this article: <http://dx.doi.org/10.1080/1573062X.2017.1325501>



© 2017 The Author(s). Published by Informa UK Limited, trading as Taylor & Francis Group



[View supplementary material](#)



Published online: 01 Jun 2017.



[Submit your article to this journal](#)



Article views: 268



[View related articles](#)



[View Crossmark data](#)



Citing articles: 1 [View citing articles](#)

## Development and validation of a drinking water temperature model in domestic drinking water supply systems

Ljiljana Zlatanovic<sup>a</sup>, Andreas Moerman<sup>b</sup>, Jan Peter van der Hoek<sup>a,c</sup>, Jan Vreeburg<sup>b,d</sup> and Mirjam Blokker<sup>b,e</sup>

<sup>a</sup>Department of Water Management, Delft University of Technology, Delft, The Netherlands; <sup>b</sup>Department of Water Infrastructure, KWR Watercycle Research Institute, Nieuwegein, The Netherlands; <sup>c</sup>Waternet, Strategic Centre, Amsterdam, The Netherlands; <sup>d</sup>Sub- department of Environmental Technology, Wageningen University, Wageningen, The Netherlands; <sup>e</sup>Department of Civil and Structural Engineering, University of Sheffield, Sheffield, United Kingdom

### ABSTRACT

Domestic drinking water supply systems (DDWSs) are the final step in the delivery of drinking water to consumers. Temperature is one of the rate-controlling parameters for many chemical and microbiological processes and is, therefore, considered as a surrogate parameter for water quality processes. In this study, a mathematical model is presented that predicts temperature dynamics of the drinking water in DDWSs. A full-scale DDWS resembling a conventional system was built and run according to one year of stochastic demands with a time step of 10 s. The drinking water temperature was measured at each point-of-use in the systems and the data-set was used for model validation. The temperature model adequately reproduced the temperature profiles, both in cold and hot water lines, in the full-scale DDWS. The model showed that inlet water temperature and ambient temperature have a large effect on the water temperature in the DDWSs.

### ARTICLE HISTORY

Received 29 November 2016  
Accepted 27 April 2017

### KEYWORDS

Drinking water; domestic systems; water temperature; modelling

### Introduction


The domestic drinking water system (DDWS) is defined as the part of the drinking water distribution system that includes plumbing between a water meter and consumer's tap, and thus, represents the final section of a drinking water supply system. Apart from being made from a wide range of materials that are not commonly present in the distribution mains (copper, brass, high-density polyethylene, stainless steel), the factors that additionally distinguish DDWSs from the distribution mains are the magnitude of residence time, temperature gradient, surface area to volume ratio and loss of disinfectant residual (NRC 2006).

Among the above-mentioned factors, temperature is one of the most important parameters affecting the quality of drinking water. The significance of drinking water temperature is based upon its role in physical, chemical and biological processes. Viscosity of drinking water, for instance, tends to fall as temperature increases. A rise from 5 to 25 °C causes the viscosity to drop by almost 40% resulting in a decrease in flow resistance, which affects the transport phenomena in pipes (Blokker and Pieterse-Quirijns 2013). Chemically speaking, water temperature is important due to its effects on copper solubility, the rate of corrosion, lead leaching from brass fixtures, bulk chlorine decay rate and formation of disinfection by-products. Higher water temperatures aggravate the corrosion of pipes. As an example, an increase in water temperature to 60 °C in copper pipes results in nearly three times higher copper levels (Singh and Mavinic 1991,

Boulay and Edwards 2001). Leaching of brass may significantly be increased by temperature rise leading to increased lead levels that leached from brass elements (Sarver and Edwards 2011). Bulk chlorine decay rates have also been found to increase with temperature, and the chlorine decay coefficient in water was reported to increase more than threefold when temperature goes from 10 to 20 °C (Li *et al.* 2003). In case of the presence of the organic precursors in drinking water, formation of chlorination by-products, as trihalomethanes (THMs), is inevitable. In a study on THMs formation it was concluded that levels of trihalomethanes increased considerably with elevation of water temperature (Li and Sun 2001). Water temperature is known to promote biological processes, as biological activity increases twofold when temperature increases by 10 °C (Van der Kooij 2003). Higher water temperatures also encourage bacterial regrowth and coliform occurrence during the water distribution phase (LeChevallier *et al.* 1996a, 1996b).

Given the substantial impact that temperature may have on water quality, the World Health Organization recommends a maximum value of 25 °C for drinking water (WHO 2006). In the Netherlands, where drinking water is being distributed without persistent disinfectant residual, the temperature of drinking water at the customers' tap is not allowed to exceed 25 °C. However, as stated in a recent study (Blokker and Pieterse-Quirijns 2013), during a relatively warm year (2006), 0.1% of the samples did exceed the legislative limit.

**CONTACT** Ljiljana Zlatanovic  l.zlatanovic@tudelft.nl

 The supplemental material for this paper is available online at <http://doi.org/10.1080/1573062X.2017.1325501>

© 2017 The Author(s). Published by Informa UK Limited, trading as Taylor & Francis Group.

This is an Open Access article distributed under the terms of the Creative Commons Attribution-NonCommercial-NoDerivatives License (<http://creativecommons.org/licenses/by-nc-nd/4.0/>), which permits non-commercial re-use, distribution, and reproduction in any medium, provided the original work is properly cited, and is not altered, transformed, or built upon in any way.

Even though the drinking water temperature has been recognized as one of the crucial parameters affecting the drinking water quality, most research on modelling of water quality in distribution systems have considered water temperature to be constant (DiGiano and Zhang 2004, Rubulis *et al.* 2007). In a recent study, a model that predicts the temperature of the water in distribution networks was proposed (Blokker and Pieterse-Quirijns 2013). To our knowledge, the temperature dynamics have not been modelled yet for the DDWSs. In this research a model, intended to predict the temperature dynamics in DDWSs, was developed and validated.

## Methodology

### Model development

#### Temperature model

The temporal change of water temperature inside the pipes is governed by the difference between water temperature and ambient temperature. Calculation of the temperature change over the time step  $\Delta t$  can be done by solving the energy balance equation for a control volume with arbitrary length  $\Delta x$ :

$$E_{T,t+\Delta t} - E_{T,t} = \Delta E_T \quad (1)$$

where  $E_{T,t}$  and  $E_{T,t+\Delta t}$  [J/m] symbolize the amount of thermal energy in the control volume at time  $t$  and time  $t+\Delta t$ , respectively, while  $\Delta E_T$  represents the change of thermal energy in the control volume over the time interval  $\Delta t$ . By introducing the geometry of the control volume and physical properties of water, the differential equation is generated:

$$\frac{dT}{dt} = \frac{4h_{\text{overall}}}{\rho c_p D} (T_\infty - T) \quad (2)$$

where  $T$  is the actual temperature of water, which is averaged over the pipe diameter, [K],  $T_\infty$  is the ambient temperature [K],  $h_{\text{overall}}$  is the overall heat transfer coefficient [ $\text{W m}^{-2} \text{K}^{-1}$ ],  $\rho$  the water density [ $\text{kg m}^{-3}$ ],  $c_p$  the heat capacity of water [ $\text{J kg}^{-1} \text{K}^{-1}$ ] and  $D$  the pipe diameter [m].

To obtain the overall heat transfer coefficient, it is essential to establish the different heat transfer processes that occur along the pipe. These processes can be divided into three phases: convective heat transfer phase inside the pipe ( $R_{\text{conv},1}$ ), conductive heat transfer phase through the pipe wall ( $R_c$ ) and convective heat transfer phase outside the pipe ( $R_{\text{conv},2}$ ) (Cengel 2002).

The overall thermal resistance can be described as Equation (3):

$$R_{\text{overall}} = R_{\text{conv},1} + R_c + R_{\text{conv},2} \quad (3)$$

The overall heat transfer coefficient can be related to the thermal resistance and can be defined as shown in Equation (4):

$$h_{\text{overall}} = \frac{1}{\frac{1}{h_{\text{water}}} + \frac{1}{h_{\text{out}}} + \frac{1}{h_{\text{wall}}}} \quad (4)$$

The variables  $h_{\text{water}}$ ,  $h_{\text{out}}$  and  $h_{\text{wall}}$  are the heat transfer coefficients for the inner ( $h_{\text{water}}$ ) and outer pipe surface ( $h_{\text{out}}$ ) and the pipe wall ( $h_{\text{wall}}$ ) in  $\text{W m}^{-2} \text{K}^{-1}$  (Cengel 2002).

The heat transfer coefficient for the inner surface of the pipe is calculated as (Cengel 2002):

$$h_{\text{water}} = \frac{\lambda_w \text{Nu}_w}{D} \quad (5)$$

where  $\lambda_w$  symbolizes the water thermal conductivity [ $\text{W m}^{-1} \text{K}^{-1}$ ] and  $\text{Nu}_w$  is the Nusselt number for water.

Depending on the flow conditions (stagnant, laminar or turbulent), the value of the Nusselt number changes (Janssen and Warmoekserken 1991):

$$\text{Nu}_w = \begin{cases} \text{Re} < 10 & 5.8 \\ 10 < \text{Re} \leq 2300 & 3.66 \\ \text{Re} > 2300 & 0.023 \text{Re}^{0.8} \text{Pr}^{1/3} \end{cases} \quad (6)$$

where  $\text{Re}$  is Reynolds number and  $\text{Pr}$  is Prandtl number.

The heat transfer coefficient for the outer surface of the pipe can be calculated by Equation (7):

$$h_{\text{out}} = \frac{\lambda_a \text{Nu}_a}{D} \quad (7)$$

where  $\lambda_a$  is the thermal conductivity of air [ $\text{W m}^{-1} \text{K}^{-1}$ ] and  $\text{Nu}_a$  is the Nusselt number for air.

The Nusselt number for air can be calculated using the Rayleigh number ( $\text{Ra}$ ), which is equal to the product of the Grashof ( $\text{Gr}$ ) and the Prandtl ( $\text{Pr}$ ) number:

$$\text{Nu}_a = \alpha \text{Ra}^\gamma = \alpha (\text{Gr} \cdot \text{Pr})^\gamma \quad (8)$$

where  $\alpha$  and  $\gamma$  are coefficients which are experimentally obtained. All pipes are treated as vertical plates in this research and  $\alpha = 0.59$  and  $\gamma = 0.26$  (Cengel 2002).

The Grashof number can be calculated as (Cengel 2002):

$$\text{Gr} = \frac{g\beta(T_\infty - T_s)G^3}{\nu^2} \quad (9)$$

where  $g$  is the acceleration of gravity [ $\text{m s}^{-2}$ ],  $\beta$  is the thermal expansion coefficient of air [ $\text{K}^{-1}$ ],  $T_s$  is the temperature at the outer pipe wall surface [K],  $\nu$  is the kinematic viscosity of air [ $\text{m}^2 \text{s}^{-1}$ ] and  $G$  is the length [m] of the characteristic geometry. Since the characteristic geometry is positioned perpendicular to the direction of the gravity force, for vertical pipes the characteristic geometry is equal to the pipe length, while for horizontal pipes  $G$  is considered to be equal to the pipe diameter.

The heat transfer coefficient for the wall of the pipe can be derived using the Equation (10):

$$h_{\text{wall}} = \frac{\lambda_p}{d_p} \quad (10)$$

where  $\lambda_p$  represents the pipe thermal conductivity [ $\text{W m}^{-1} \text{K}^{-1}$ ] and  $d_p$  is the thickness of the pipe wall [m], which is considered to be 10% of the pipe diameter in this research.

While water flows in pipes, air flow develops around the pipes, and thus, Nusselt numbers are averaged along the characteristic geometry for which the Nusselt number equals (Cengel 2002):

$$\text{Nu}_a = 0.59 \text{Ra}^{0.25} \quad (11)$$

Substituting Equations (5), (7) and (11) in Equation (4) and assuming  $d = 0.1D$  we end up with the Equation (12):

$$h_{\text{overall}} = D(\lambda_w^{-1} \text{Nu}_w^{-1} + 0.1\lambda_p^{-1} + \lambda_a^{-1} \text{Nu}_a^{-1}) \quad (12)$$

## Hydraulic model

To model the temperature dynamics in DDWSs it is essential to have: (1) information on the lay-out of the system to be modelled, in terms of pipe diameters, lengths of pipes and pipe materials; (2) a set of demand patterns for each tap point in the systems; (3) a hydraulic simulation software; (4) an extension to the hydraulic software to implement the equations from the temperature model.

In this research, the layout of the DDWSs was done according to a plan of a terraced house, so-called Typical Dutch House (Supplemental Figure S1), as terraced houses account for approximately 62% of all residential properties in The Netherlands (as cited in Majcen *et al.* 2013)

The demand patterns were generated by SIMDEUM (**S**IMulation of water **D**emand, an **E**nd **U**se **M**odel) for a two-person household. SIMDEUM, developed by KWR Watercycle Research Institute (Nieuwegein, The Netherlands), is a stochastic model which is grounded on statistical information of water appliances and water consumers. SIMDEUM generates water demand patterns based on consumers' behaviour, considering the differences in DDWSs and water appliances (Blokke *et al.* 2006, 2010). In total, 365 different demand patterns for a two-person household (including 104 weekend patterns) were generated.

Modelling the hydraulics within the DDWSs was done by applying a free water distribution system modelling software EPANET. EPANET was developed by the United States Environmental Protection Agency (EPA) in 1993 (Rossman 2000). The simulation outputs provide hydraulic information such as, flows in pipes, pressures and water residence times at various locations in the systems.

An extension to EPANET called EPANET-MSX (**M**ulti-**S**pecies **e**Xtension), was used to implement the temperature model equations. This extension uses a Lagrangian time-based approach, i.e. 'follows' the trajectory of water parcels throughout the system and considers concentrations, in this case temperature, as a function of time and their prior coordinates.

## Model validation

### Experimental rig

To validate the temperature model (and to study the influence of the DDWS's extension for fire sprinklers system integration, which is a topic of a parallel research carried out by the authors), two full-scale test rigs were built using standard copper pipes. One experimental rig was built in a way to resemble a conventional DDWS, while the other was constructed with the extension of the plumbing for the residential sprinkler accommodation. In this paper, only the results from the conventional DDWS rig are presented.

The rigs were located in an old elevator shaft at the Water Laboratory of the Faculty of Civil Engineering and Geoscience at the Delft University of Technology and they were directly connected to the drinking water line in the Water Laboratory. The distance between the connection point to the drinking water supply line and the beginning of the test rigs at the water meters was 40 m. The 40-m supply pipe with a diameter of 35 mm was insulated using 10 mm Armaflex AF2 insulation foam, with thermal conductivity of  $33 \text{ W}\cdot\text{m}^{-1}\cdot\text{K}^{-1}$  (12 times smaller than copper thermo conductivity).

Configuration of the conventional experimental rig, which was used for model validation (Supplemental Figure S1), complies with the Dutch home plumbing codes NEN 1006 (NEN1006 2002). The conventional DDWSs consisted of two vertical lines and four horizontal branches of copper (manufactured in accordance with European Standard EN 1057), namely vertical copper composite of 22 mm diameter – carrying cold water to the upper floors, vertical copper tube of 15 mm (ID) – delivering hot water from a 50-L water heater and copper tubing's of 15 mm- supplying cold and hot water from the vertical lines to the 11 plumbing fixtures (solenoid valves), as given in Supplemental Figure S2. The total length of the pipes was 48.6 m in the conventional system and the volume of the plumbing rig was 6 L.

### Water consumption pattern

To be able to mimic a realistic drinking water consumption at the household level, the test rigs included 11 solenoid valves (point of use) per system. The valves were configured to run automatically ('on' and 'off' mode) according to one-year demand patterns with a time step of 10 s, which were generated by SIMDEUM model. For the sake of validation of the temperature model, a SIMDEUM pattern for a weekend day was used. In Supplemental Figure S3 the measured flows are given.

In the DDWS experimental rig, the magnetic valves operated only in 'on' and 'off' mode. This means that the valves were either fully open or fully closed, which is not common in real DDWSs. In addition to this, in experimental DDWSs opening a tap to the full extent took longer than in real water systems (from 'off' to 'on' mode – the magnetic valve response is 0.1–4 s). What was also specific for the experimental set-up is that all magnetic valves were of the same discharge capacity of 4 tapping units (TU), where capacity of 1 TU is equal to 5 L/min. Having a slow response and the same capacity for all valves in the systems resulted in larger discharge on the weekend day, as the total measured daily water use was 1000 L.

The length of the pipe that delivers water from the connection point to the lab rigs is 40 m. Despite the fact that the pipe has been thermo-insulated, stagnant water in the pipe heated up by  $2.5 \text{ }^\circ\text{C}$  per hour, until it got equal to the ambient temperature. For the purpose of model validation, the 40-m long pipe was flushed for 5 min before the opening of each tap in the system. This was done in order to ensure a stable inlet water temperature profile, for the purpose of drinking water temperature model validation.

Every point of use in the systems was equipped with a flow sensor and a temperature probe. A temperature probe was also mounted before the water meters, to measure the inlet water temperature. Moreover, three ambient temperature sensors were installed on every 'floor' of our virtual Typical Dutch House. Before starting the experiments, all sensors were manually calibrated. The drinking water temperatures, ambient temperatures and flows were continuously measured, every 10 s. The ambient temperature around the pipes was also manually measured three times a day during the 'model validation' day. The control of the solenoid valves and data logging was achieved by using the data acquisition, control and analysis software LabView.

### Overview of the input parameters

The overview of the parameters used to validate the temperature model is given in Table 1.



## Statistical analysis

The goodness of fit between measured and modelled values was assessed using the following statistical measures: standard regression (correlation coefficient (R)), dimensionless (Nash-Sutcliffe efficiency (N-S)) and error measurements (root mean square error (RMSE)) (Nash and Sutcliffe 1970, Willmott *et al.* 1985).

The correlation coefficient indicates the strength of a linear relationship between the model outputs and observed values. The correlation coefficient is derived by dividing the covariance of the two variables by the product of their standard deviations, as given by Equation (13):

$$R = \frac{\sum_{i=1}^n (x_i - \bar{x}) \cdot (y_i - \bar{y})}{\sqrt{\sum_{i=1}^n (x_i - \bar{x})^2 \cdot \sum_{i=1}^n (y_i - \bar{y})^2}} \quad (13)$$

where  $x_i$  are the observed and  $y_i$  are the modelled values and  $\bar{x}$  and  $\bar{y}$  refer to the sample mean values.

The value of the correlation coefficient ranges from  $-1$  to  $+1$ . If  $R = 0$ , there is no linear relationship between the simulated and observed values, while if  $R = 1$  or  $-1$ , there is a perfect positive or a perfect negative linear relationship between the variables.

The Nash-Sutcliffe efficiency N-S is used to evaluate hydrologic models and to study the ability of a model to reproduce the verification data-set (Nash and Sutcliffe 1970). This coefficient is calculated as shown in Equation (14):

$$N - S = 1 - \frac{\sum_{i=1}^n (y_i - x_i)^2}{\sum_{i=1}^n (x_i - \bar{x})^2} \quad (14)$$

Nash-Sutcliffe efficiencies are found in the range from  $-\infty$  to 1. An efficiency of 1 ( $N-S = 1$ ) shows a perfect fit between simulated and measured values. An efficiency of lower than zero suggests that the mean value of the measured data would have been a better predictor than the model itself.

As for the error index, root mean square error (RMSE) – which is described as the mean of the squares of errors, is commonly used in model evaluation. This error measurement is valuable because it indicates the extent of error among the simulated and measured values. RMSE is calculated based on Equation (15):

$$RMSE = \sqrt{\frac{\sum_{i=1}^n (x_i - y_i)^2}{n}} \quad (15)$$

A RMSE value of 0 indicates a perfect goodness of fit.

## Sensitivity analysis

In order to identify the most relevant parameters involved in the DDWS temperature model, a sensitivity analysis was carried out. The sensitivity analysis included a variation of the selected input parameters by 10% from their initial values. The selected input parameters for water were: temperature of influent water ( $T_w$ ), thermal conductivity ( $\lambda_w$ ), Prandtl number ( $Pr_w$ ) and heat capacity ( $c_p$ ). The selected input parameters for air were: ambient temperature ( $T_\infty$ ), thermal conductivity ( $\lambda_a$ ), Prandtl number ( $Pr_a$ ) and thermal expansion coefficient  $\beta$ , while thermal conductivity of copper pipes ( $\lambda_p$ ) was selected for the sensitivity analysis for the pipes. The percentage of the output difference was measured for the data-set at the kitchen tap.

**Table 1.** Overview of the parameters used in the DDWS temperature model.

Parameter	Symbol	Value	Unit	Source
<b>Water</b>				
Temperature of influent water	$T_w$	9	°C	Measured
Thermal conductivity at 15 °C	$\lambda_w$	0.589	W·m <sup>-1</sup> ·K <sup>-1</sup>	Cengel 2002
Prandtl number at 15 °C	$Pr_w$	8.09	–	Cengel 2002
Heat capacity	$c_p$	4185	J·kg <sup>-1</sup> ·K <sup>-1</sup>	Cengel 2002
<b>Air</b>				
Ambient temperature	$T_\infty$	14.5–16	°C	Measured
Thermal conductivity at 15 °C	$\lambda_a$	0.02476	W·m <sup>-1</sup> ·K <sup>-1</sup>	Cengel 2002
Prandtl number at 15 °C	$Pr_a$	0.7323	–	Cengel 2002
Thermal expansion coefficient at 15 °C	$\beta$	0.00349	K <sup>-1</sup>	<a href="http://www.mhlt.uwaterloo.ca">http://www.mhlt.uwaterloo.ca</a>
Kinematic viscosity at 15 °C	$\nu$	$1.47 \times 10^{-5}$	m <sup>2</sup> ·s <sup>-1</sup>	Cengel 2002
<b>Pipes</b>				
Thermal conductivity of copper pipes	$\lambda_p$	403	W·m <sup>-1</sup> ·K <sup>-1</sup>	Cengel 2002

## Results and discussion

A graphical visualization of the simulated and measured values can give a first valuable feedback whether the model outcomes are realistic. Figure 1 depicts measured flows and temperature profiles for the kitchen tap in the experimental rig.

As can be seen from Figure 1, the dynamics of the measured temperatures are predicted well by the temperature model for

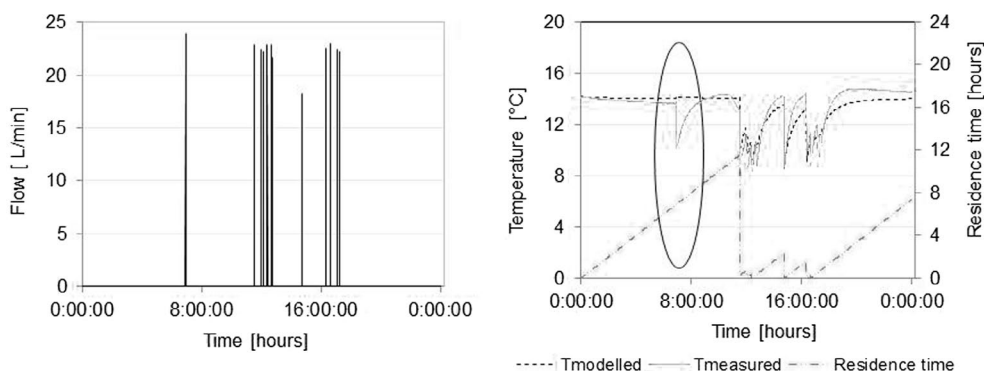


**Figure 1.** Left: Flow measured at the kitchen tap. Right: Modelled and measured temperature profiles at the kitchen tap plus modelled water residence time in the system.

DDWSs. However, some irregularities were spotted, i.e. where no temperature drop was predicted by the model, but was measured in the rig (see the ellipse in Figure 1). No change in the residence time was also observed at the same interval, which indicates that EPANET didn't recognize the measured extraction of water at the kitchen tap around 07:30 in the morning.

The explanation for this phenomenon is that the hydraulic network solver EPANET was primarily designed to predict the hydraulics within a drinking water distribution system (Rossman 2000). Drinking water distribution systems consist of pipes with larger diameters, longer pipe sections and higher water flows compared to a DDWS. In the hydraulic models of DDWSs, apart from small diameters (13 mm), the lengths between the junctions and the tap points are as small as  $\sim 1$  m. Thus, the mathematical engine most likely starts losing the power to converge accurately with flows over a single time step (10 s), resulting in non-recognition of the real water consumption. To overcome this drawback, an attempt was made to tune the flow input.

The tuning of the input flow included the process of determining best estimates for unknown flows by comparing model outcomes and measured temperature record. Wherever the irregularities between modelled and measured temperatures were found, the measured input demand patterns were manually modified by:

- (1) assigning 10 s of the additional flow of the same magnitude
- (2) distributing the flow over a shorter time step, i.e. 5 s.

The graphical visualization of the results and the cumulative probability curves that were generated before and after tuning the input flow are presented in Figure 2.

As is evident from Figure 2, both addition of supplementary flows of 10 s ( $T_{\text{modelled-tuned flow } 10\text{s}}$  in Figure 2) and distributing the flow over 5 s ( $T_{\text{modelled-tuned-flow } 5\text{s}}$  in Figure 2) result in more adequate trends of the temperature profiles for kitchen cold tap. This implies that better hydraulic performance in EPANET 2.0 was accomplished with the aid of the flow adjusting procedure.

Validation was also done for hot water line as is given in Figure 2 (bottom). Because the demands of the hot bathroom tap were long enough ( $> 20$  s), the pattern was not tuned by assigning extra flows. However, an additional simulation was done with tuned 5 s time step, to assess the difference in temperature profiles if shorter time steps are applied. Graphical comparison, presented in Figure 2 shows that the model is able to adequately reproduce temperature profiles at the hot water taps, as well.

The ability of the temperature model to reproduce the temperature dynamics in DDWSs was assessed by statistical measures, applying the raw and tuned flow input, shown in Table 2.

Table 2 shows that tuning the flow input improved model performance in terms of all three statistical measures for cold water line. The values of both correlation coefficient – R and

**Table 2.** Statistical measures for temperature model performance.

Flow input	R	N-S	RMSE
<i>Cold water tap</i>			
Raw data – time step 10 s	0.822	0.662	0.867
Tuned flow input – time step 10 s	0.899	0.783	0.695
Tuned flow input – time step 5 s	0.923	0.809	0.651
<i>Hot water tap</i>			
Raw data – time step 10 s	0.978	0.955	1.384
Tuned flow input – time step 5 s	0.982	0.955	1.382

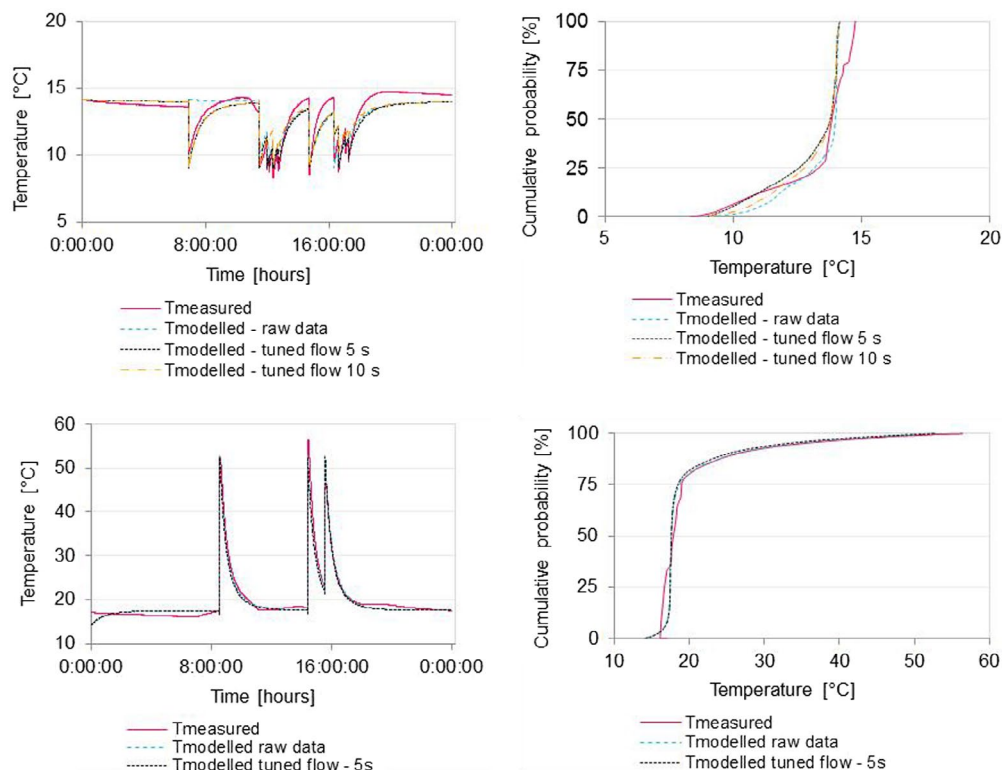


**Figure 2.** Water temperature profiles and cumulative probability curves for observed and simulated data at the kitchen cold water tap (up) and bathroom sink hot water tap (down).

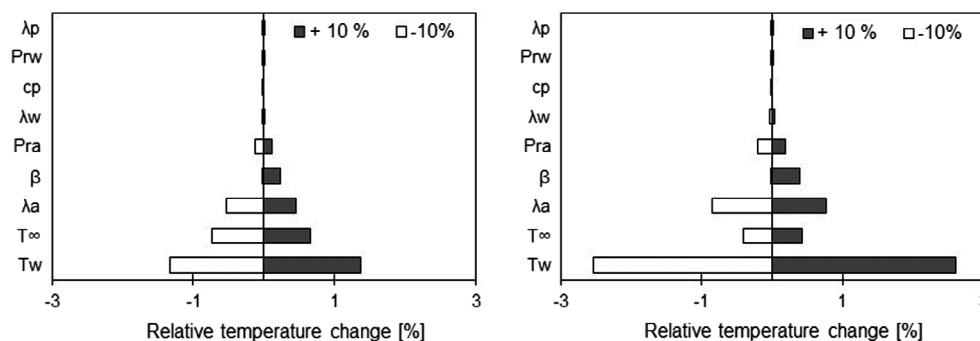


**Figure 3.** Sensitivity of the water temperature model to the input parameters. Left Model outputs for all day simulation. Right Model outputs during extraction hours (from 06.00 to 19:00).

Nash-Sutcliffe efficiency N-S increased (from 0.822 to 0.923 and from 0.662 to 0.809, respectively) while the error index, RMSE, decreased from 0.867 to 0.651. In general, model prediction can be judged as 'very good' if  $N-S > 0.70$  and  $R > 0.90$ , as for the error indices that are represented in the units of the temperature ( $^{\circ}\text{C}$  or K), error values close to zero indicate perfect fit. According to Singh *et al.* (2004) if RMSE is smaller than one-half of a standard deviation of measured time series, RMSE can be judged as low. In our case, the standard deviation value was 1.49, implying that the error index may be considered low for models with tuned flow.

We need to mention that discrepancies between measured and modelled results were observed in the hours with no flow. This was expected, as the ambient temperature fluctuates by a few degrees on a daily basis, while the model assumes constant ambient temperature. The discrepancies also had an effect on the statistical parameters. If the data during the daytime with no flow are excluded from the statistical analysis (from 00:00 to 6:00 and from 19:00 to 00:00), R and N-S were improved to 0.937 and 0.992, respectively, while RMSE was of the same order, 0.704.

For the hot water line, the simulation with the tuned flow over the time step of 5 s yielded only slightly better statistical parameters (Table 2), whereas R was improved from 0.978 to 0.982, while RMSE and N-S were in the same order, 0.955 and 1.382 (1.384), respectively. Here again, excluding the hours without the demand from the statistical analysis (from 00:00 to 6:00 and from 19:00 to 00:00), resulted in improved R and N-S values to 0.984 and 0.999, respectively, while RMSE was found to be larger (1.748), but still the value of RMSE was found to be less than one-half of the standard deviation of the measured time series (6.478).

Even though the statistical measures for the temperature modelling when employing tuned hydraulic models are satisfactory, one must bear in mind that it is of high importance to have a model with limited errors in terms of hydraulics. Thus, to obtain representative results when having single step demands, it is necessary to assess whether or not EPANET recognized the flow, which can be done by analysing the extent of residence time at a given flow.

The measured and modelled data revealed that the water temperature dynamics in homes is mainly driven by the water consumption pattern. Both modelled and measured data (measured data are given in Supplemental Figure S4) showed that drinking water is being warmed up by 0.5 to 2  $^{\circ}\text{C}$  within the copper DDWSs, namely from the inlet point to the tap in use, depending on how far from the inlet point the demand takes

place (Supplemental Figure S3). Therefore, if the drinking water temperature is determined by sensors in drinking water distribution networks, the temperatures at the points of use can be underestimated.

The sensitivity analysis (Figure 3 (left)) for all-day simulation data revealed that the most relevant parameters are the temperature of inlet water ( $T_w$ ), the temperature of air ( $T_\infty$ ) and the thermal conductivity of air ( $\lambda_a$ ). If only extraction hours are included in the sensitivity analysis (from 06.00 to 19:00), the inlet water temperature is found to play a more important role, as variation of  $\pm 10\%$  in the input temperature leads to  $\pm 2.5\%$  of relative change in the output temperature (Figure 3 (right)). Here again, the most sensitive parameters were found to be the temperature of inlet water, the temperature of air and the thermal conductivity of air, and, hence, these values need to be put in the model with high accuracy. From the sensitivity analysis it can be concluded that, when modelling water temperature in DDWSs, the most important transfer process is the exchange process of heat between water and air through the pipe wall.

In the conducted research, DDWS made of copper was used for the model validation. Because the model is based on fundamental thermodynamic principles, it can be used for other DDWSs pipe materials as well. Nevertheless, the applicability of the model for other pipe materials which are commonly applied in DDWSs needs to be experimentally validated. If the temperature model shows the same accuracy for the other pipe materials, it would be possible to couple the temperature model for DDWSs with a model that predicts the temperature of the water in the drinking water distribution system, fulfilling the goal to model the temperature dynamics from the treatment facilities (reservoirs) to the points of actual water use (drinking water taps in DDWSs).

## Conclusion

A temperature model for DDWSs was developed, by integration of a temperature model, a hydraulic model and a demand pattern model (SIMDEUM). A combination of graphical and statistical techniques was used for model evaluation. A statistical analysis showed that the model is able to adequately predict the temperature profiles within DDWSs. The most sensitive parameters in the model are the temperature of the inlet water, the temperature of air and the thermal conductivity of air, implying the most dominant transfer process is the (convective) heat



exchange between water and air through the pipe wall. Because the model is based on fundamental thermodynamic principles, it is believed that this model can be used for other pipe materials which are used in DDWSs.

## Disclosure statement

No potential conflict of interest was reported by the authors.

## Funding

The authors would like to acknowledge financial support from Dutch Automatische bluswatersystemen project (Agentschap Project No. IMV1100047), Stichting PIT, and drinking water companies Waternet, Vitens, Oasen, PWN and Brabant Water.

## References

- Blokker, M. and Pieterse-Quirijns, E.J., 2013. Modeling temperature in the drinking water distribution system. *Journal American Water Works Association*, 105 (1), 35–36.
- Blokker, E.J.M., Vreeburg, J.H.G., and Vogelaar, A.J., 2006. *Combining the probabilistic demand model SIMDEUM with a network model*. Cincinnati, OH: Water Distribution Systems Analysis Symposium, 1–11.
- Blokker, E.J.M., Vreeburg, J.H.G., and van Dijk, J.C., 2010. Simulating residential water demand with a stochastic end-use model. *Journal of Water Resources Planning and Management*, 136 (1), 19–26.
- Boulay, N. and Edwards, M., 2001. Role of temperature, chlorine, and organic matter in copper corrosion by-product release in soft water. *Water Research*, 35 (3), 683–690.
- Cengel, Y., 2002. *Heat transfer: A practical approach*. New York: McGraw-Hill.
- DiGiano, F.A. and Zhang, W., 2004. Uncertainty analysis in a mechanistic model of bacterial regrowth in distribution systems. *Environmental Science & Technology*, 38 (22), 5925–5931.
- Janssen, L.P. and Warmoekserken, M.M., 1991. *Transport phenomena data companion*. Uitgevers Maatschappij b.v.
- LeChevallier, M.W., Shaw, N.J., and Smith, D.B., 1996a. *Factors limiting microbial growth in distribution systems: Full-scale experiments*. Denver, CO: American Water Works Association.
- LeChevallier, M.W., Welch, N.J., and Smith, D.B., 1996b. Full-scale studies of factors related to coliform regrowth in drinking water. *Applied and Environmental Microbiology*, 62 (7), 2201–2211.
- Li, X.Z. and Sun, J.M., 2001. Further formation of trihalomethanes in drinking water during heating. *International Journal of Environmental Health Research*, 11 (4), 343–348.
- Li, X., et al., 2003. Modeling of residual chlorine in water distribution system. *Journal of Environmental Sciences*, 15 (1), 136–144.
- Majcen, D., Itard, L.C.M., and Visscher, H., 2013. Theoretical vs. actual energy consumption of labelled dwellings in the Netherlands: Discrepancies and policy implications. *Energy Policy*, 54, 125–136.
- Nash, J.E. and Sutcliffe, J.V., 1970. River flow forecasting through conceptual models part I – A discussion of principles. *Journal of Hydrology*, 10 (3), 282–290.
- NEN1006, 2002. *General requirements for water supply installations*. Delft, The Netherlands: Nederlands Normalisatie instituut (NEN).
- NRC, 2006. *Drinking water distribution systems: Assessing and reducing risks*. Washington, DC: The National Academies Press.
- Rossman, L.A., 2000. *EPANET 2 user manual*. Cincinnati: Water Supply and Water Resources Division, National Risk Management Research Laboratory, Cincinnati, OH.
- Rubulis, J., et al., 2007. Methodology of modeling bacterial growth in drinking water systems. D 5.5.4. Techneau, Riga (2007).
- Sarver, E. and Edwards, M., 2011. Effects of flow, brass location, tube materials and temperature on corrosion of brass plumbing devices. *Corrosion Science*, 53 (5), 1813–1824.
- Singh, I. and Mavinic, D.S., 1991. Significance of building and plumbing specifics on trace metal concentrations in drinking water. *Canadian Journal of Civil Engineering*, 18 (6), 893–903.
- Singh, J., et al., 2004. Hydrological modeling of the Iroquois river watershed using HSPF and SWAT1. *Journal of the American Water Resources Association*, 41 (2), 343–360.
- Van der Kooij, D., 2003. *Managing regrowth in drinking water distribution systems. Heterotrophic plate counts and drinking-water safety*. London, United Kingdom: IWA Publishing, 199–232.
- WHO, 2006. *Guidelines for drinking-water quality; Incorporating first addendum to third edition*. Geneva: World Health Organization.
- Willmott, C., et al., 1985. Statistics for the evaluation and comparison of models. *Journal of Geophysical Research*, 90, 8995–9005.